An Experimental Study of Bubble Rise Characteristics in non – Newtonian (Power-Law) Fluids

N. M. S. Hassan [1], M. M. K. Khan[1], M. G. Rasul[1] and D.W. Rackemann[2]

[1]College of Engineering and Built Environment
Faculty of Sciences, Engineering and Health
Central Queensland University, Rockhampton, Queensland, 4702, AUSTRALIA

[2]Sugar Research and Innovation
Queensland University of Technology, Brisbane, Queensland, 4001, AUSTRALIA

Abstract

Air bubbles are used in chemical, biochemical, environmental, food process such as sugar industries for improving the heat and mass transfer. In particular, the bubble rise characteristics in massecuite - a fluid made from sugar crystals and sugar syrup have a great influence on vacuum pan operation which is an important process for the production of raw sugar in sugar industries. An experimental study of the bubble rise characteristics in xanthan gum solutions, a non-Newtonian (Power-Law) massecuite equivalent fluid are presented in this paper. The main characteristics, i.e. the bubble velocity, the bubble trajectory, and the drag relationship were investigated as a function of volume of air bubbles. The bubble rise velocity and trajectory were measured using a combination of non-intrusive (high speed photographic) method and digital image processing. The parameters that significantly affect the rise of air bubble are identified. The effect of different bubble volumes and liquid heights on the bubble rise velocity and bubble trajectory are analysed and discussed. A relationship between the Reynolds number and the drag coefficient is presented and discussed.

Introduction

In sugar factories, cane or beet juice is evaporated into concentrated syrups. The syrup is concentrated further and crystallized into sugar by boiling in large vessels called vacuum pans. The vacuum pans are seeded with small sugar crystals and the sugar solution is kept supersaturated to encourage the seed crystals to grow to a desired size by adding more syrup while controlling the boiling conditions. This process is called crystallization. During the boiling process, vapour bubbles are formed in the sugar solution and rise to the surface. The vapour bubbles serve to mix the solution to maintain homogeneity and suspend the sugar seed crystals in solution, so that the seeds do not settle on the bottom of the vacuum pan.

When the crystals reach the required size in the vacuum pan, the mixture (known as massecuite) is discharged. Massecuite refers to the crystal-suspension mixture which comprises of sugar crystals surrounded by a mother syrup (known as molasses). The molasses is separated from the massecuite in centrifugals and the separated molasses is boiled again to recover more sucrose through crystallisation. It results when sucrose is crystallized out of the juice/syrup solution. The crystallization process has the effect of concentrating the impurities in the molasses. The impurities (polysaccharides, waxes, gums, etc) enter the sugar factory as small concentrations in the juice.

Massecuites and molasses generally demonstrate non-Newtonian flow behaviour; that is the viscosity depends on the rate of shear which is well defined by the Power-Law model. The molasses and massecuites have approximately the same degree of shear thinning behaviour in terms of Power-Law index [1]. The Power-Law index, n, of massecuite lies between 0.5 and unity with values further removed from unity representing a more pronounced pseudoplastic behaviour which is shown in table 1.

Authors	No of exp	Temp, ^{0} C	Crystal content	Size range mm	Shear rate, s^{-1}	Power Law index
Done, 1950	12	40 -50	15 – 45	0.3 – 0.8	0.1 – 1.5	0.85 ± 0.04
Adkins, 1951	5	room	20 -40	n.a.	0.1 – 4	0.60 – 0.90
Nicklin, 1958	36	room	5 -30	0.3 – 2.1	0.1 – 4	0.90 ± 0.05
Kot et al., 1968	-	20 -30	15 -50	0.2 – 0.4	1 -30	0.8 – 1.0
Awang and White, 1976	22	30 -60	15 - 30	0.3	2 - 100	0.92 ± 0.07

Table 1. Investigation of pseudoplastic behaviour of massecuites [2].

The detailed measurements have demonstrated that massecuites show pseudo-plastic behaviour at lower shear stress; that is the viscosity is highest at low shear rates and decreases with increasing shear rates [2,3,4]. On the other hand, there has been speculation that low grade massecuites (lowest purity) are not purely viscous but also exhibit viscoelastic properties [5,6,7].

The apparent viscosity of a massecuite depends on the shear rate, temperature, the properties of the molasses and the crystal. Three types of massecuites are found in Australian sugar factories, namely A, B and C massecuites. These massecuites are distinguished on the basis of their sucrose concentration or purity. A massecuite (high grade massecuite) has the highest purity and C massecuite (low grade massecuite) has the lowest purity. The decrease in purity of the massecuites results from the recycle of molasses streams in the crystallization process to improve sugar recovery. The viscosity of massecuites increases with the level of impurities, hence A massecuites have the lowest viscosity. This study is focused on A massecuite as it produces the main product of sugar factories. The typical values of viscosity of A massecuites for Australian sugar cane conditions range from 1 Pa.s - 2 Pa.s at the start of an A massecuite cycle up

to 15 Pa.s - 30 Pa.s when the A massecuite is discharged from the pan [8].

Massecuites are not optically clear so the study of bubble rise characteristics in massecuite fluids, it is essential to simulate the massecuite with an equivalent non-Newtonian fluid which is optically clear and has similar rheological properties to the massecuite. Furthermore the examination of massecuite fluids in a non-factory environment is inherent with problems namely degradation during storage and changing rheological properties under different temperature conditions. Due to these issues, a range of stable and optically clear non-Newtonian polymer solutions were considered and characterized instead of using massecuite fluids.

This study examines the bubble characteristics as they rise through a non-Newtonian fluid. The rise of a bubble in a liquid is a function of several parameters namely, bubble characteristics (size and shape), properties of gas-liquid systems, liquid motion (direction), and operating conditions. The most significant characteristics of air bubbles are the bubble rise velocity or terminal velocity, trajectory and the drag co-efficient. The drag co-efficient correlates the drag force exerted on a moving air bubble to its terminal velocity and projected surface area. The terminal velocity of an air bubble is termed as the velocity attained at steady state conditions where all applied forces are balanced. The bubble rise velocity and drag co-efficient for an air bubble are dependent on the liquid and bubble properties.

There is limited literature on bubble rise characteristics in massecuite equivalent non-Newtonian Power-Law fluids. More research and in–depth analysis on bubble rise phenomena in non-Newtonian fluid is necessary as most industrial fluids prevalent in chemical, biochemical, environmental and food processes are non-Newtonian in nature. The main aim of this study is to investigate the bubble rise velocity and trajectory in massecuite equivalent non-Newtonian Power-Law fluids. The drag co-efficient correlation of the bubble is compared with the results of other analytical and experimental studies available in the literature.

Experimental Set-up and Procedure
Experimental Test Rig
The experimental set up selected in this study was similar to that used by Dewsbury et al. [9]. The experimental apparatus is shown schematically in figure 1.
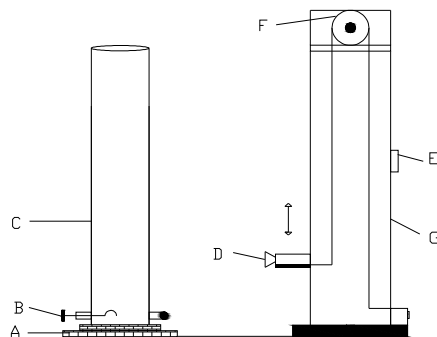

Figure 1. Schematic diagram of experimental apparatus.
A = Sturdy Base; B = Rotating Spoon; C = Cylindrical test rig (0.125 m diameter), D = Video camera; E = Variable speed motor; F = Pulley; and G = Camera lifting apparatus.

The rig consists of a polycarbonate tube approximately 1.8 m in height and 0.125 m in diameter. The bubble insertion mechanism consists of a ladle or spoon that has the capability to control the injection of air.

The camera lifting apparatus stands approximately 2.0 m high to allow the movement of the camera mount device to move through roughly 1.8 m in height.

The variable speed drive of the camera lifting apparatus regulates the control of the camera mount device. This drive allows the camera to be raised at approximately the same velocity as the bubble.

A high speed digital video camera (Panasonic, NV-GS11, 24X optical Zoom) was mounted on the camera mount device with a small attachment to the side of the camera lifting apparatus.

Bubble Rise Velocity Measurement
Bubble rise velocities were computed by a frame by frame analysis of successive images. The bubble images were analysed with the software Windows Movie Maker by recording the bubble rise time and measuring the velocity.

Bubble Diameter Measurement
A bubble equivalent diameter was measured from the still frames obtained from the video image. The still images were then processed using "SigmaScan Pro 5.0" commercial software and the bubble height (d_h) and bubble width (d_w) were measured in pixels. The pixel measurements were converted to millimetres based on calibration data for the camera. The bubble equivalent diameter, d_{eq} was determined [10] as

$$d_{eq} = \left(d_h \times d_w^{\,2} \right)^{\frac{1}{3}}$$

(1)

where d_w is the long axis length and d_h is the short axis length of the bubble. For this measurement it was assumed that the bubble was axi-symmetric with respect to its short axis direction.

Bubble Trajectory Measurement
Bubble trajectory was determined from the still images collected from the digital video camera by analysing the pixel location of the bubble images in the still frames.

Reynolds Number and Drag Co-efficient Calculation
Since the fluid viscosity varies as a function of the shear rate so the terminal velocity of the bubble (U_b) also changes with the change in shear rate. The average shear rate over the entire bubble surface is equal to (U_b/d_b) so the apparent viscosity (μ) can be written [11,12] as

$$\mu = K \left(U_b / d_b \right)^{n-1}$$

(2)

where d_b = the characteristic diameter of the bubble, m

K = the consistency of the fluid, Pa.s^n. The higher the value of K the more viscous the fluid.

n = flow index, dimensionless.

In the case of spherical bubble, the Reynolds number (Re) for non-Newtonian Power-Law fluid was defined as

$$\mathrm{Re} = \frac{\rho_{liq} d_b^n U_b^{2-n}}{K}$$

(3)

For a non-spherical bubble with a vertical axis of symmetry, the Re was termed [9,11,12,13] by

$$\mathrm{Re} = \frac{d_w^n U_b^{2-n} \rho_{liq}}{K}$$

(4)

The drag co-efficient for spherical bubble was calculated by

$$C_d = \frac{4gd_b\Delta\rho}{3\rho_{liq}U_b^2}$$

(5)

In the case of non-spherical bubble, the drag co-efficient was computed by

$$C_d = \frac{4gd_{eq}^3\Delta\rho}{3\rho_{liq}d_w^2U_b^2}$$

(6)

The drag co-efficient for non-spherical bubbles were analysed on the basis of the real bubble geometry in equation (6), where d_{eq} is the equivalent sphere diameter and d_w is the diameter of the horizontal projection of bubble or long axis length of the bubble and $\Delta\rho$ is the density difference between the liquid and the air.

Material Used

Several combinations of different concentrations of polymer solutions (including a number of polyacrylamides and xanthan gums) mixed with water were tested for the selection of the massecuite equivalent non-Newtonian fluid. The xanthan gum solutions exhibited shear thinning pseudoplastic behaviour and showed the greatest similarities to the rheological properties of massecuites. As such, xanthan gum solutions were used in this study to simulate the properties of massecuite solutions. The fluids studied included water solutions mixed with concentration of 0.025%, 0.05% and 0.1% of xanthan gum (by weight). The temperature of all solutions in this study was maintained at 25^0 C in a temperature controlled room. For every solution, the measured density of the solution was very close to the density of water at 25^0 C since they were made with low concentrations of xanthan gum in the liquid.

Fluid Characterisation

The rheological properties for different concentration of the various xanthan gum solutions tested are illustrated in figure 2 and summarized in table 2.
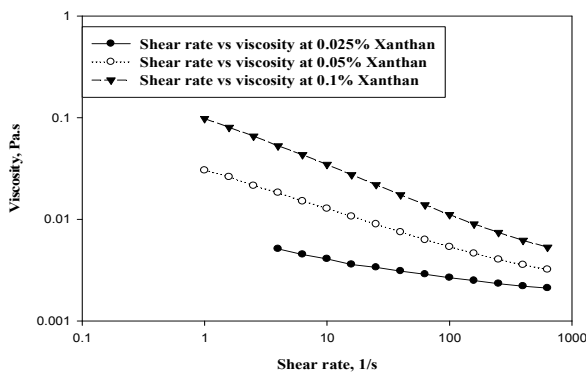

Figure 2. Viscosity vs. shear rate of xanthan gum solutions demonstrating the pseudoplastic behaviour.

Fluid Type	Concentration (%)	K, $Pa.s^n$	n	Density, kg/m^3
Xanthan gum	0.025	0.00612	0.8248	996.0
Xanthan gum	0.05	0.03024	0.6328	996.0
Xanthan gum	0.1	0.09503	0.5481	997.0

Table 2. Rheological and physical properties of xanthan gum solutions.

Rheological properties of the solutions were measured using an ARES (Advanced Rheometric Expansion System) rheometer. The range of shear rates to determine fluid rheology was 1 s^{-1} - 650 s^{-1}.

Figure 2 shows that the polymer (xanthan gum) solutions exhibit non-Newtonian shear-thinning pseudoplastic behaviour which is adequately illustrated by Power-Law model as follows

$$\eta = K\dot{\gamma}^{n-1}$$

(7)

where η = non-Newtonian viscosity, Pa.s

$\dot{\gamma}$ = shear rate, s^{-1}.

The flow curve of xanthan gum solution (0.1% xanthan gum by weight) was found at lower shear rate range to be showing similar to that of high grade massecuite. But the density of this solution was found relatively low in comparison with massecuite solutions since it was very hard to match both viscosity and density of the simulation fluid. However, the viscous effect of the xanthan gum solutions were more pronounced than elastic effects and this phenomenon was similar to that observed with high grade massecuite solutions.

Results and Discussion
Bubble Rise Velocity

The bubble velocity was measured at a location of 1.0 m above the point of air injection for the three different concentrations of xanthan gum solutions for various bubble volumes (0.1mL - 5.0mL) and the results are illustrated in figure 3. It is seen from the figure 3 that for the bubbles of 5.0mL volume, the bubble velocity (0.30 m/s) is very similar for all three xanthan gum solutions when measured at 1 m height. For the smaller bubble volumes (0.1mL and 0.2mL) the viscous forces are more dominant and a small decrease in bubble velocity for increasing solution viscosity can be observed. For larger bubble volumes (1mL, 2mL and 5mL), as the solution viscosity increases the viscous forces have a less dominant on the terminal motion and terminal rise velocity.

The effect of the viscous forces can also be seen as the Re increases with increasing bubble volume. Viscous forces do not dominate the bubble velocity at high Re. For high Re, the inertia forces dominate the motion of the bubble [14]. In this region (>0.2mL bubble size), the bubble rise velocity increases with the equivalent diameter of the bubble. This increase in velocity can also be explained by the bubble internal circulation that reduces the drag co-efficient due to a reduction in the friction at the gas-liquid interface [9]. However the internal circulation of the bubble does not affect the drag co-efficient to the same extent at low Re as evidenced by the limited increase in bubble velocity between the bubbles of volume of 0.1mL and 0.2mL in figure 3.
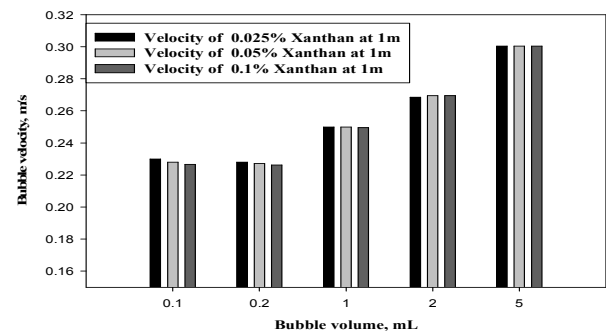

Figure 3. Velocity profile for different concentrations of xanthan gum solutions at 1m height.

The velocity profile of the xanthan gum solutions for various bubble volumes (0.1-5.0mL) are illustrated in figure 4 when measured at different liquid heights in the test apparatus. Figure 4 shows the same phenomena as is observed in figure 3. It can be observed from figure 4 that the average bubble velocity slightly decreases with the increase in liquid height but not to a significant extent, though the pressure changes with the increase in height is very small.
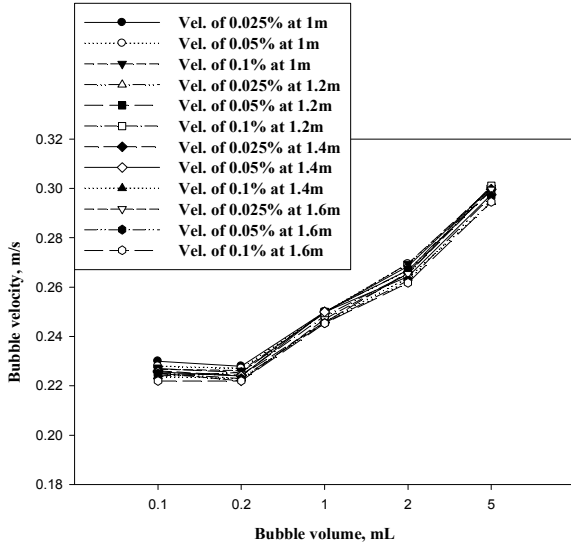

Figure 4. Velocity profile for different concentrations of xanthan gum solutions at different heights.

Bubble Trajectory

The trajectory results of three different concentrations of xanthan gum solutions are shown in figure 5 for bubbles of size 0.1mL and 5.0mL when measured over a distance of 1.0 m height from the point of air injection. From figure 5, it can be observed how the bubble trajectory becomes more scattered which is described by the standard deviation of the data. This standard deviation is the distance from the vertical line above the bubble release point. When the bubble was released, the general trend was for the bubble to remain close to the release centre and as it rose through the liquid, it spread out as the height increases.
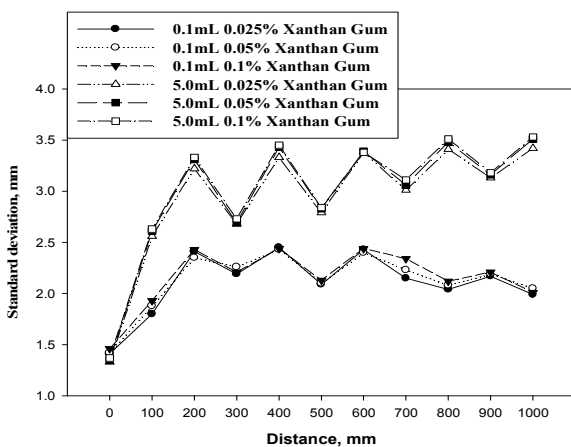

Figure 5. Standard deviation of the trajectory as bubble moves upwards of bubbles in three different xanthan gum solutions (0.1mL and 5.0mL bubble).

For the three different xanthan gum solutions, the 0.1mL bubble had a lower standard deviation and hardly differed from their alignment with the release point which was seen from their

reasonably straight standard deviation shown in figure 5. For the larger bubbles (5.0mL) at the three different concentrations, the spread was much broader than the 0.1mL bubbles. This phenomenon is completely opposite to that of water where the small bubbles deviate more than the larger bubbles [15]. At low Re (smaller bubble of 0.1mL), the rising bubble showed a linear trajectory. At high Re, the larger bubble of 5.0mL volume displayed a spiral trajectory because the effect of wake shedding influenced the bubble to induce a spiralling rising motion. In the xanthan gum solutions, the horizontal motion of the 0.1mL bubbles is reduced due to less friction acting upon their surface compared to the larger bubbles and so the smaller bubbles experience less resistance to vertical movement. But larger bubbles experience more resistance on top and deform as their size increases that result in spiral motion.

Drag Co-efficient

For low Re (<0.1), the creeping flow regime, the bubble velocity is dependant on the viscosity of the fluid and the gas bubble follows Hadamard-Ryczynski model at very low Re rather than Stokes model due to the internal circulation of the gas bubble which is given [16] by

$$C_d = \frac{16}{Re}$$

(8)

where C_d is the drag co-efficient. As expected, model (8) fails in high Reynolds number when the current experimental data was compared.

The widely accepted correlation of the drag co-efficient for solid particles proposed by Turton and Levenspiel [17] is as follows,

$$C_d = \frac{24}{Re}\left(1 + 0.173\,Re^{0.657}\right) + \frac{0.413}{1 + 16,300\,Re^{-1.09}}$$

(9)

Equation (9) converges to Stokes model at low Re. A modified correlation was suggested for gas bubbles in non-Newtonian Power-Law fluids [9] valid for any value of Re, and is given by

$$C_d = \frac{16}{Re}\left(1 + 0.173\,Re^{0.657}\right) + \frac{0.413}{1 + 16,300\,Re^{-1.09}}$$

(10)

Equation (10) converges to the Hadamard -Rybczynski equation, at low Re.

The experimental and predicted bubble drag co-efficient of equations (9) and (10) are presented in figures 6, 7 and 8 as a function of Re for solutions with xanthan gum concentrations of 0.025%, 0.05% and 0.1% respectively. The experimental bubble drag co-efficient were calculated based on equations (5) or (6) depending on the shape of the bubble. It is noted that no universal drag curve for the case of rising air bubbles in non-Newtonian Power-Law fluids has been developed yet in the available literature.

In figure 6, the deviation of the experimental C_d was seen initially higher than the predicted values by equations (9) and (10) across the Re range investigated but this deviation reduced with increasing Re.

The same phenomenon was observed from figure 7 in that the deviation of the experimental C_d was higher in comparison with the equations (10) over the entire Re range investigated but the experimental C_d correlated better with equation (9) at higher Re.

It can be observed from figure 8 that the experimental C_d showed reasonable agreement with equations (9) and (10).
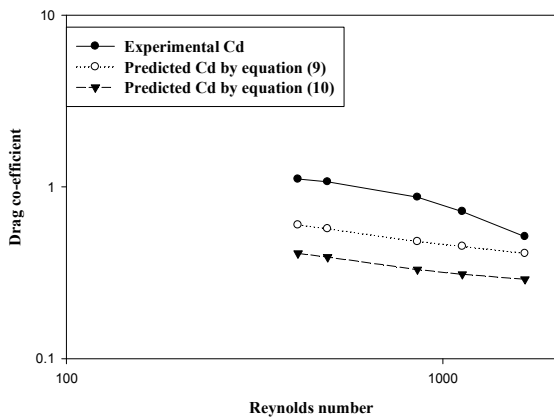

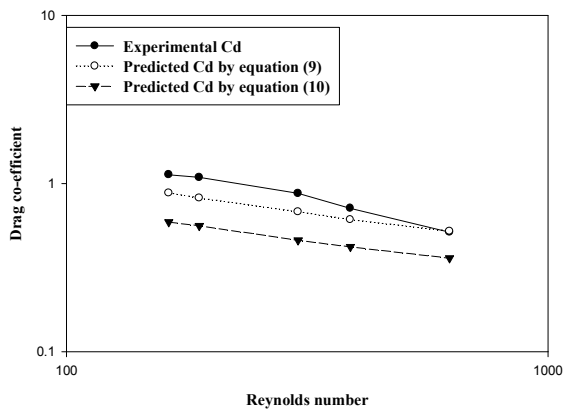Figure 6. Drag co-efficient vs. Reynolds number for rising air bubble in 0.025% xanthan gum solution.

Figure 7. Drag co-efficient vs. Reynolds number for rising air bubble in 0.05% xanthan gum solution.

The deviation of the experimental C_d was higher in comparison with equation (9) at high Re but was less at lower Re indicating the gas bubble follows the Hadamard -Rybczynski equation rather than Stokes model. Therefore, it can be concluded that the published literature is capable of giving a fair prediction for the bubble drag co-efficient for solutions of higher concentrations of xanthan gum.
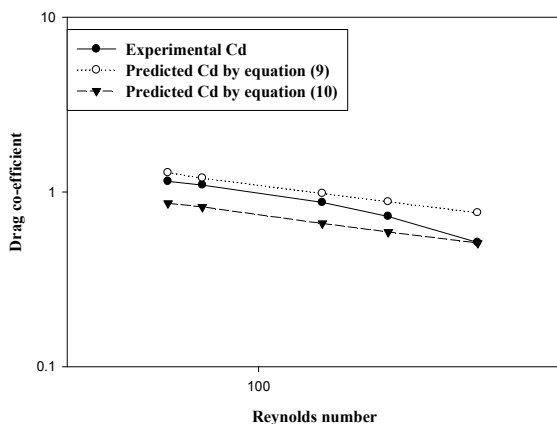

Figure 8. Drag co-efficient vs. Reynolds number for rising air bubble in 0.1% xanthan gum solution.

Conclusions

A new experimental set-up was used to analyse the characteristics of the bubbles rising in different concentration of xanthan gum solutions. The bubble rise characteristics, namely, bubble velocity, trajectory and drag coefficient produced acceptable and consistent results.

The bubble rise phenomena showed how the bubble velocity varies with the increase in bubble volume as the bubble rises through liquid column. The velocity profile elucidated a trend for different concentrations of xanthan gum solutions that the average bubble rise velocity increases with the increase in bubble volume. For smaller bubble volumes (0.1mL and 0.2mL) the viscous forces are more dominant and a small decrease in bubble velocity for increasing solution viscosity can be observed. The average bubble velocity slightly decreases when measured with an increase in liquid height above the air injection point for corresponding bubble volumes.

The trajectory results demonstrated the general trend of the bubble. As the bubble size increases, the trajectory spread also increases for the different xanthan gum solutions. This is due to the change in the resistance on the rising bubbles, the increase in viscosity and the deformation in bubble shape.

The relationship between C_d-Re for non-Newtonian Power-Law fluids showed acceptable results with the available analytical and experimental studies of the literature with better results obtained for higher viscosity solutions.

As the xanthan gum solutions do not fully replicate the properties of massecuite solutions, further study is warranted to develop a more suitable transparent solution to simulate typical massecuite mixtures.

References

[1] Broadfoot, R. and Miller, K. F., Rheological Studies of Massecuites and Molasses, Int. Sugar Jnl., **92** (1098), 1990, 107-112.

[2] Awang, M. and White, E. T., Effect of Crystal on the Viscosity of Massecuites, Proc. Qld Soc. Sugar Cane Technol., **43**, 1976, 263-270

[3] Adkins, B. G., Proc. Qld Soc. Sugar Cane Technol., **18**, 1951, 43-52.

[4] Done, W. G., Flow Properties of Massecuites, PhD Thesis, 1950, University of Queensland.

[5] Leong, Y. K., McBain, G. D., Chu, S. Y. and Ong, B. C., Pseudo-plastic and Viscoelastic Behaviour of Molasses, Proc. Aust. Soc. Sugar Cane Technol., **23**, 2001, 341-345.

[6] McBain, G. D., Harris, J. A., Leong, Y. K. and Vigh, S., Viscoelastic Characterisation of Low-Grade Molasses by Jet-Swell Measurements, Proc. Aust. Soc. Sugar Cane Technol., **22**, 2000, 467-473.

[7] Ness, J. N., On the Measurement of Massecuite Flow Properties, Proc. Int. Soc. Sugar Cane Technol., **18**, 1983, 1295-1303.

[8] Rackemann, D. W., Evaluation of Circulation and Heat Transfer in Calandria Tubes of Crystallisation Vacuum Pans, M.Eng.Sc Thesis, 2005, James Cook University.

[9] Dewsbury, K., Karamanev, D. G. and Margaritis, A., Hydrodynamic Characteristics of Free Rise of Light Solid Particles and Gas Bubbles in Non-Newtonian Liquids, Chemical engineering Science, **54**, 1999, 4825-4830.

[10] Lima-Ochoterena, R. and Zenit, Visualization of the Flow Around a Bubble Moving in a Low Viscosity Liquid, Revista Mexicana De Fisica, **49** (4), 2003, 348-352.

[11] Lali, A. M., Khare, A. S., Joshi, J. B. and Nigam, K. D. P., Behaviour of Solid Particles in Viscous non-Newtonian Solutions: Settling Velocity, Wall Effects and Bed Expansion in Solid-Liquid Fluidized Beds, Powder Technology, **57**, 1989, 39-50.

[12] Margaritis A., te Bokkel, D. W. and Karamanev, D. G., Bubble Rise Velocities and Drag Coefficients in non-Newtonian Polysaccharide solutions, 1999, John Wiley & Sons, Inc.

[13] Miyhara, T. and Takahashi, T., Drag Coefficient of a Single Bubble Rising through a Quiescent Liquid, Int. Chem. Eng., **25** (1), 1985.

[14] Kulkarni, A. A. and Joshi, J. B., Bubble Formation and Bubble Rise Velocity in Gas-Liquid Systems: A Review, Ind. Eng. Chem. Res., **44,** 2005, 5873-5931.

[15] Hassan, N. M. S., Khan, M. M. K. and Rasul, M. G., A Comparative Study of Bubble Rise Phenomena in Water and Low concentration Polymer Solutions, HEFAT 2007, Heat Transfer, Fluid Dynamics and Thermodynamics – 5th international Conference, Sun City, South Africa, July, 1-4, 2007.

[16] Miyahara, T. and Yamanaka, S., Mechanics of Motion and Deformation of a single Bubble Rising through Quiescent Highly Viscous Newtonian and non-Newtonian Media, Jnl Chem. Eng., **26** (3), 1993, 297-302.

[17] Turton, R., and Levenspiel, O., A short note on the Drag Correlation for Spheres, 1986, Powder Technology.